Evaluation of type 2 diabetic mellitus animal models via interactions between insulin and mitogen-activated protein kinase signaling pathways induced by a high fat and sugar diet and streptozotocin

JUNCHENG ZHUO[1,2*], QIAOHUANG ZENG[3*], DAKE CAI[2], XIAOHUI ZENG[2], YUXING CHEN[2], HAINING GAN[2], XUEJUN HUANG[2], NAN YAO[2], DANE HUANG[2] and CHENGZHE ZHANG[1,2]

[1]Department of Pharmacology of Traditional Chinese Medicine, The Fifth Clinical Medical College, Guangzhou University of Chinese Medicine, Guangzhou, Guangdong 510095; [2]Guangdong Provincial Key Laboratory of Research and Development in Traditional Chinese Medicine, Guangdong Province Engineering Technology Research Institute of TCM, Guangzhou, Guangdong 510405; [3]Department of Chinese Medicine Immunity, The Second Affiliated Hospital of Guangzhou University of Chinese Medicine, Guangzhou, Guangdong 510006, P.R. China

Received March 31, 2017; Accepted October 13, 2017

DOI: 10.3892/mmr.2018.8504

Abstract. Type 2 diabetic mellitus (T2DM), which is characterized by insulin resistance (IR), hyperglycemia and hyperlipidemia, is a comprehensive dysfunction of metabolism. The insulin receptor (INSR)/phosphoinositide 3-kinase (PI3K)/AKT signaling pathway is well acknowledged as a predominant pathway associated with glucose uptake; however, the effect of streptozotocin (STZ) plus a high fat and sugar diet (HFSD) on the proteins associated with this pathway requires further elucidation. In order to explore this effect, a T2DM rat model was constructed to investigate T2DM pathogenesis and potential therapeutic advantages. Rats were randomly divided into control and model groups, including normal diet (ND) and HFSD types. ND types were administered intraperitoneal (IP) injections of STZ (35 mg/kg) or a combination of STZ and alloxan monohydrate (AON) (40 mg/kg), whereas HFSD types were composed of HFSD pre-given, post-given and simul-given groups, and were modeled as follows: IP or intramuscular (IM) injection of STZ (35 mg/kg) or a combination of STZ and AON (40 mg/kg). Results indicated that, compared with controls, blood glucose, insulin, homeostatic model assessment-insulin resistance and total triglyceride were significantly elevated in groups with HFSD and modeling agents ($P<0.05$ or $P<0.01$), whereas total cholesterol and low-density lipoprotein levels were significantly elevated in groups simultaneously administered HFSD and modeling agents ($P<0.05$ or $P<0.01$), in addition to downregulation of the expression of insulin signaling pathway proteins in the liver, including INSR, PI3K, AKT1, phosphatidylinositol-5-phosphate 4-kinase type-2α (PIP5Kα) and glucose transporter (GLUT)2, and increased expression of inflammatory factors, including p38, tumor necrosis factor (TNF) α and interleukin (IL)6. Furthermore, compared with other two HFSD types including pre-given and post-given group, the simul-given group that received IM injection with STZ exhibited decreased expression levels of major insulin signal pathway proteins INSR, PI3K, AKT1, PIP5Kα, GLUT2 or GLUT4 in the liver and pancreas ($P<0.05$ or $P<0.01$), whereas the opposite was observed in the skeletal muscle. In addition, the protein expression levels of phosphorylated-p38, p38, IL6 and TNFα in the simul-given group that received IM injection with STZ were increased ($P<0.05$ or $P<0.01$), and histopathology also indicated inflammation in pancreas and liver. The present findings suggest that a low dose of STZ may partially impair the β cells of the pancreas, whereas long-term excess intake of HFSD may increase lipid metabolites, inhibit the insulin signaling pathway and activate the mitogen-activated protein kinase p38 signaling pathway. The combined action of STZ and AON may result in insulin resistance, which ultimately results in abnormalities in glucose and lipid metabolism. The present model, analogue to T2DM onset of humans, evaluated the medical effect on metabolic dysfunction and provides an insight into the underlining mechanism of IR.

Correspondence to: Dr Xiaohui Zeng or Mr. Yuxing Chen, Guangdong Provincial Key Laboratory of Research and Development in Traditional Chinese Medicine, Guangdong Province Engineering Technology Research Institute of TCM, 60 Hengfu Road, Yuexiu, Guangzhou, Guangdong 510405, P.R. China
E-mail: 227050896@qq.com
E-mail: cyx89333@qq.com

*Contributed equally

Key words: type 2 diabetic mellitus, insulin resistance, mitogen activated protein kinase, insulin signal pathway, protein expression

Introduction

In recent years, type 2 (T2) diabetic mellitus (DM) has accounted for 90-95% of DM cases and the incidence has markedly increased. It has been estimated that >347 million people suffer from DM globally and the number is expected to double to ~694 million by 2030 (1). Numerous complications are associated with T2DM, including blindness, kidney failure and cardiac dysfunction (2-4). Therefore, the mechanism of T2DM and the identification of potential effective treatments have been fervently investigated.

According to previous research, multiple methods have been proposed for the construction of T2DM models, including the use of transgenic animals and induction with chemical agents (5,6). Streptozotocin (STZ) selectively destroys islet β cells, is used extensively in establishing T2DM animal models (7,8) and may be administered intramuscularly or intraperitoneally. However, the extent of islet β cell damage is dose-dependent (9). Following investigation of STZ dosage, 35 mg/kg has been identified as the optimal dosage of STZ to induce DM (10,11). Furthermore, increased doses of STZ have been associated with increased mortality in animals (12). Alloxan monohydrate (AON) is another chemical agent that has been demonstrated to interfere with islet energy production, and 40 mg/kg of AON has been suggested to establish a diabetic rat model (13). Recently, a high fat and sugar diet (HFSD) with administration of STZ has been suggested to establish a T2DM rat model, and it has been reported that models induced by diet variations rather than genetic factors may represent a more true mechanism of DM pathogenesis (14).

The insulin-mediated insulin receptor (INSR)/phosphoinositide 3-kinase (PI3K)/protein kinase B (AKT) signaling pathway is widely known as a primary pathway associated with the regulation of glucose uptake (15). During insulin resistance (IR), proteins associated with this signaling pathway are abnormally modified, which may therefore serve as intracellular markers for hypoglycemia (16,17). HFSD has also been suggested to induce dysfunction in lipid metabolism (18). In addition, previous studies have revealed that an HFSD results in free fatty acid accumulation, which may be toxic and trigger the mitogen activated protein kinase (MAPK) inflammation signaling pathway, resulting in the increase of interleukin (IL)6 and tumor necrosis factor (TNF)α, which may lead to insulin signaling pathway damage, exacerbating IR (1).

In previous studies (5-8), various models have been designed that consist of chemical agents, including STZ and AON plus HFSD. In the present study, it was hypothesized that the model may be further verified for stability from the numerous alterations of protein expression in the INSR/PI3K/AKT pathway and levels of IL6 and TNFα.

Materials and methods

Reagents. STZ (purity, >98%) and AON were obtained from Sigma-Aldrich (Merck KGaA, Darmstadt, Germany). Rat insulin ELISA kits (KA3811) were purchased from Thermo Fisher Scientific, Inc. (Waltham, MA, USA). Total cholesterol (TC; A111-1), triglyceride (TG; A110-1), glucose (GLU; F006), high-density lipoprotein cholesterol (HDL; A112-1) and low-density lipoprotein cholesterol (LDL; A113-1) enzymatic assay kits were all obtained from Nanjing Jiancheng Bioengineering Institute (Nanjing, China). Homeostatic model assessment-insulin resitance (HOMA-IR) was calculated as fasting blood GLU x fasting insulin/22.5. Accu-Chek Active test strips were purchased from Roche Diabetes Care (Bella Vista, Australia). Radioimmunoprecipitation assay (RIPA) buffer was obtained from BestBio (Shanghai, China). The BCA protein assay kit was obtained from Thermo Fisher Scientific, Inc. Mouse monoclonal anti-β-actin (A5441), anti-GAPDH (ab9484), anti-INSR (ab131238), anti-insulin receptor substrate 1 (IRS1) (ab66153), anti-PI3K (ab191606), anti-AKT1 (ab32505), anti-phosphatidylinositol-5-phosphate 4-kinase type-2 (PIP5K2) α (ab109128), anti-glucose transporter (GLUT)2 (ab54460), anti-GLUT4 (ab188317), anti-p38 (ab27936), anti-TNFα (ab6671), anti-IL6 (ab6672) and goat anti-rabbit IgG H&L horseradish peroxidase (ab97051) antibodies were purchased from Abcam (Cambridge, UK). Peroxidase-conjugated affinipure goat anti-mouse IgG (SA00001-1) antibody was purchased from ProteinTech Group, Inc., (Chicago, IL, USA). Anti-phosphorylated (p)-p38 antibody (4631) was purchased from Cell Signaling Technology, Inc., (Danvers, MA, USA).

Animals and diets. All animal experimental protocols were approved by the Animal Ethics Committee of Guangdong Provincial Engineering Technology Institute of Traditional Chinese Medicine (Guangzhou, China). The treatment of the animals was in accordance with International Guiding Principles for Biomedical Research Involving Animals (19). A total of 120 male Wistar rats (age, 8 weeks) weighing between 180 and 220 g were purchased from the Guangdong Medical Laboratory Animal Center (Guangzhou, China). All animals were maintained in a temperature-controlled room at 24±2˚C with a relative humidity of 60±10%, a 12-h light/dark cycle and had *ad libitum* access to food and water. The formula of HFSD consisted of 20% sucrose, 12% lard oil, 5% milk powder, 2% egg and 61% normal fodder.

Following acclimatization for one week, animals were divided randomly into control and model groups (Fig. 1). The control group was fed a normal diet (ND) and not exposed to any other treatments. The model group was further divided into the ND and HFSD types. Furthermore, HFSD types were designed into HFSD pre-given, post-given and simul-given types, which resulted in a total of 12 groups (n=10 in each). ND rats were administered STZ alone (35 mg/kg) or a combination of STZ (35 mg/kg) and AON (40 mg/kg) via intraperitoneal (IP) injection, and HFSD groups were administered STZ (35 mg/kg) alone via intramuscular (IM) or IP injection or a combination of STZ and AON (40 mg/kg) via IP injection. ND groups were fed a normal diet for 8 weeks, whereas HFSD rats were fed an HFSD in different periods, including pre-given, post-given and simul-given. HFSD pre-given rats were fed with HFSD for 4 weeks, induced with respective modeling agents and subjected to an HFSD for a further 4 weeks. Conversely, HFSD post-given rats were administered the respective modeling agent, and subjected to 4 weeks of ND, which was then replaced with an HFSD for the following 4 weeks. Additionally, the simul-given rats were induced with modeling agents and subjected to a HFSD for 8 weeks. STZ or the combination of STZ and AON were administered only once.

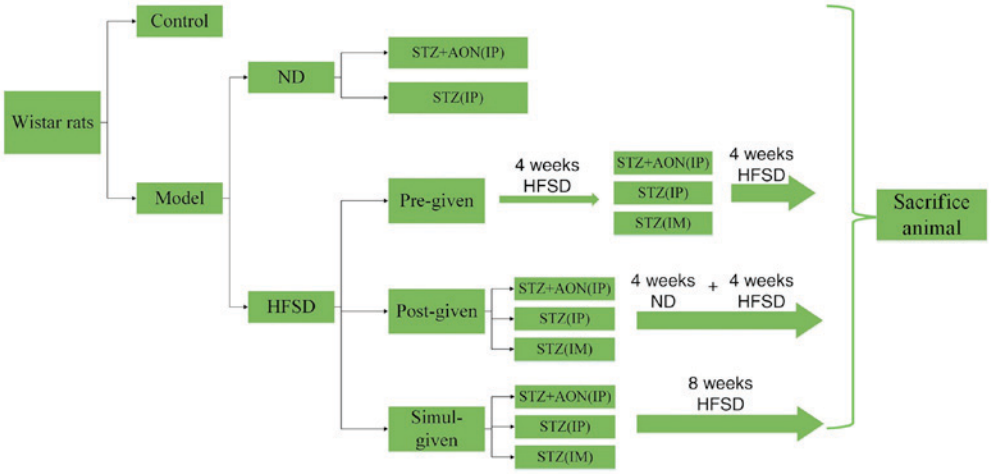

Figure 1. Type 2 diabetes mellitus rat model group design. A total of 120 Wistar rats were grouped into control and model groups. The model group was divided into ND types, which consisted of STZ+AON (IP) and STZ (IP) groups. HFSD types contained HFSD pre-, post- and simul-given groups. Each HFSD type was modeled using three methods, IP or IM injection of STZ alone or combination of STZ and AON via IP injection. A total of 12 groups were constructed (n=10 per group). IP, intraperitoneal; IM, intramuscular; ND, normal diet; AON, alloxan monohydrate; STZ, streptozotocin; HFSD, high fat and sugar diet.

Following a total of 8 weeks, the rats were anaesthetized, blood samples were collected and biochemical analysis was conducted. Rats were subsequently sacrificed and organs, including the liver, skeletal muscle and pancreas, were isolated from animals and weighed. The liver and pancreas were prepared for pathological examination, whereas the skeletal muscle and other remaining organs were stored at -80˚C prior to biochemical detection and western blot analysis.

Blood sample preparation. Blood samples (500 μl) were collected from the abdominal aorta, allowed to clot for 30 min at room temperature and then centrifuged at 3,000 x g and 25˚C for 10 min to obtain the serum, which was stored at -80˚C prior to experimental utilization.

Western blot analysis. A total of 100 mg liver, pancreas or skeletal muscle tissue was homogenized in RIPA buffer for 10 min and centrifuged at 4,000 x g for 5 min at 4˚C. Subsequently the supernatant was transferred to a centrifuge tube and the concentration of the total protein was determined via BCA protein assay. Aliquots of supernatants consisting of 45 μg protein were used to evaluate the expression of INSR, IRS1, PI3K, AKT, PIP5K2α, GLUT2, GLUT4, p38, TNFα and IL6. The samples (45 μg/lane) were subjected to 10% SDS-PAGE and were electrotransferred to a polyvinylidene difluoride membrane, which was soaked in methanol for 90 min. The membrane was blocked with skimmed milk (5%) prepared in Tris buffered saline with Tween-20 (TBST) for 60 min at 25˚C. Subsequently, the membrane was washed four times (5 min each) in TBST at 25˚C, and incubated with primary antibodies, including 1:2,000 diluted solutions of β-actin (loading control), GAPDH (loading control), anti-INSR, anti-IRS1, anti-PI3K, anti-AKT1, anti-PIP5K2α, anti-GLUT2, anti-GLUT4, anti-p38, anti-p-p38, anti-TNFα and anti-IL6 overnight at 4˚C. The membrane was washed a further three times (5 min each time) in TBST, incubated in a solution of horseradish peroxidase-conjugated anti-mouse IgG or anti-rabbit IgG secondary antibody (1:5,000 dilution) at 25˚C for 1 h, washed 3 times (5 min each time) in TBST, and then exposed to enhanced chemiluminescence reagent (EMD Millipore, Billerica, MA, USA) according to the manufacturer's instructions. The films were scanned and analyzed using a Tanon 5200 Imaging system (Tanon Science and Technology Co., Ltd., Shanghai, China).

Histological analysis. The liver and pancrease tissue were fixed in 10% neutral-buffered formalin overnight at 25 ˚C, and dehydrated in alcohol and xylene, respectively. Dehydrated samples were embedded in paraffin and cut into sections (4 μm). The sections were stained with hematoxylin and eosin (H&E) for 2 and 4 min separately at 25˚C. Morphological changes were subsequently observed with light microscopy at x40 and x200 magnification.

Statistical analysis. All data were analyzed using SPSS 22.0 (IBM Corp., Armonk, NY, USA) and were processed via one-way analysis of variance. Following analysis of variance, the Student-Newman-Keuls (for homogenous data) or Dunnett's (for non-homogenous data) post hoc tests were performed. $P<0.05$ was considered to indicated a statistically significant difference. Data are presented as the mean + standard deviation.

Results

Establishment of models increases weight, liver ratio and pancreas ratio. Body weight, liver ratio and pancreas ratio were obtained following 8 weeks of experiment. As indicated in Fig. 2, body weight and liver ratio in all model groups were increased compared with the control. Furthermore, in the majority of cases this difference was statistically significant ($P<0.05$ or $P<0.01$; Fig. 2A and B, respectively). Notably, body weight and liver ratio in HFSD groups that received STZ IP injections alone were significantly increased compared with the ND group administered STZ alone ($P<0.05$ or $P<0.01$). Additionally, the pancreas ratio in model groups was significantly reduced compared with control group ($P<0.05$ or $P<0.01$; Fig. 2C). Notably, the pancreas ratio in HFSD simul-given

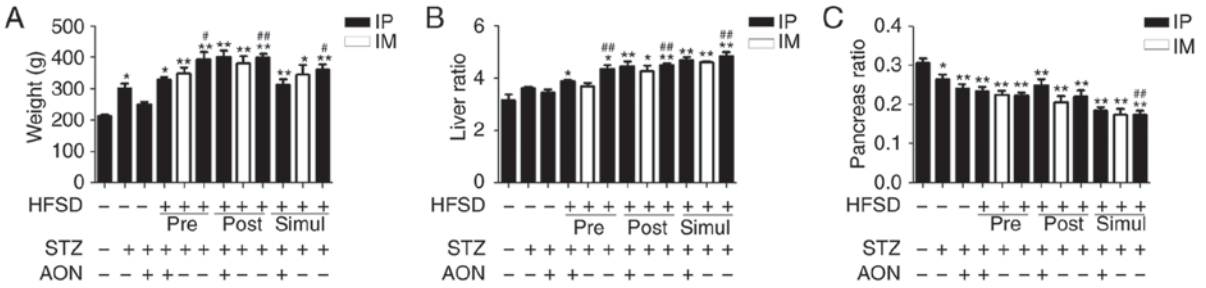

Figure 2. Body weight and relative organ ratio of type 2 diabetes mellitus rat model. (A) Body weight, (B) liver ratio and (C) pancreas ratio were determined following 8 weeks of treatment. Values are presented as the mean + standard deviation (n=10). *P<0.05 or **P<0.01 vs. control group; $^{\#}$P<0.05 or $^{\#\#}$P<0.01 vs. ND group given STZ alone. IP, intraperitoneal; IM, intramuscular; ND, normal diet; AON, alloxan monohydrate; STZ, streptozotocin; HFSD, high fat and sugar diet.

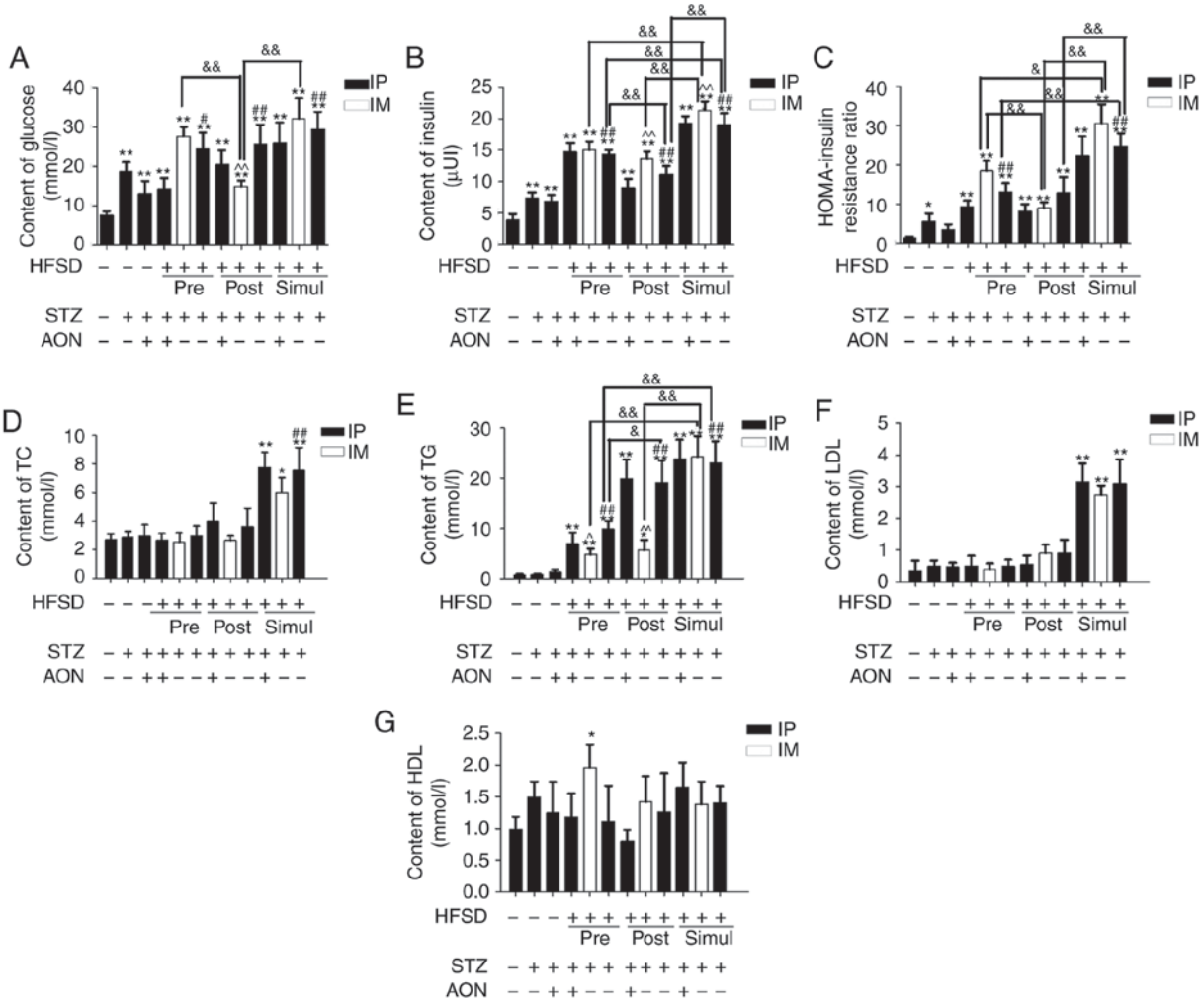

Figure 3. Relative chemical indexes of type 2 diabetes mellitus rat model. (A) Glucose, (B) insulin, (C) HOMA-insulin resistance ratio, (D) TC, (E) TG, (F) LDL and (G) HDL were detected in the sera of rats in all groups. Values are presented as the mean + standard deviation (n=10). *P<0.05 or **P<0.01 vs. control group; $^{\#}$P<0.05 or $^{\#\#}$P<0.01 vs. ND group given STZ alone; $^{\&}$P<0.05 or $^{\&\&}$P<0.01; and ^P<0.05 or ^^P<0.01 vs. HFSD groups given STZ alone via IP. IP, intraperitoneal; IM, intramuscular; ND, normal diet; AON, alloxan monohydrate; STZ, streptozotocin; HFSD, high fat and sugar diet; LDL, low density lipoprotein; HDL, high density lipoprotein; TC, total cholesterol; TG, total triglyceride; HOMA, homeostatic model assessment.

groups that received STZ IP injections was significantly reduced compared with the ND group administered STZ alone (P<0.01). However, there was no significant difference among HFSD groups in body weight, liver ratio and pancreas ratio. These findings indicated that HFSD is associated with body weight, liver and pancreas impairment.

Alteration of glucose and lipid levels in T2DM models. Serum was collected and glucose and lipid levels were detected. Compared with the control group, the blood glucose, insulin and homeostatic model assessment-insulin resitance (HOMA-IR) ratio were increased in all model groups, and in all but the ND STZ+AON group with respect to the HOMA-IR

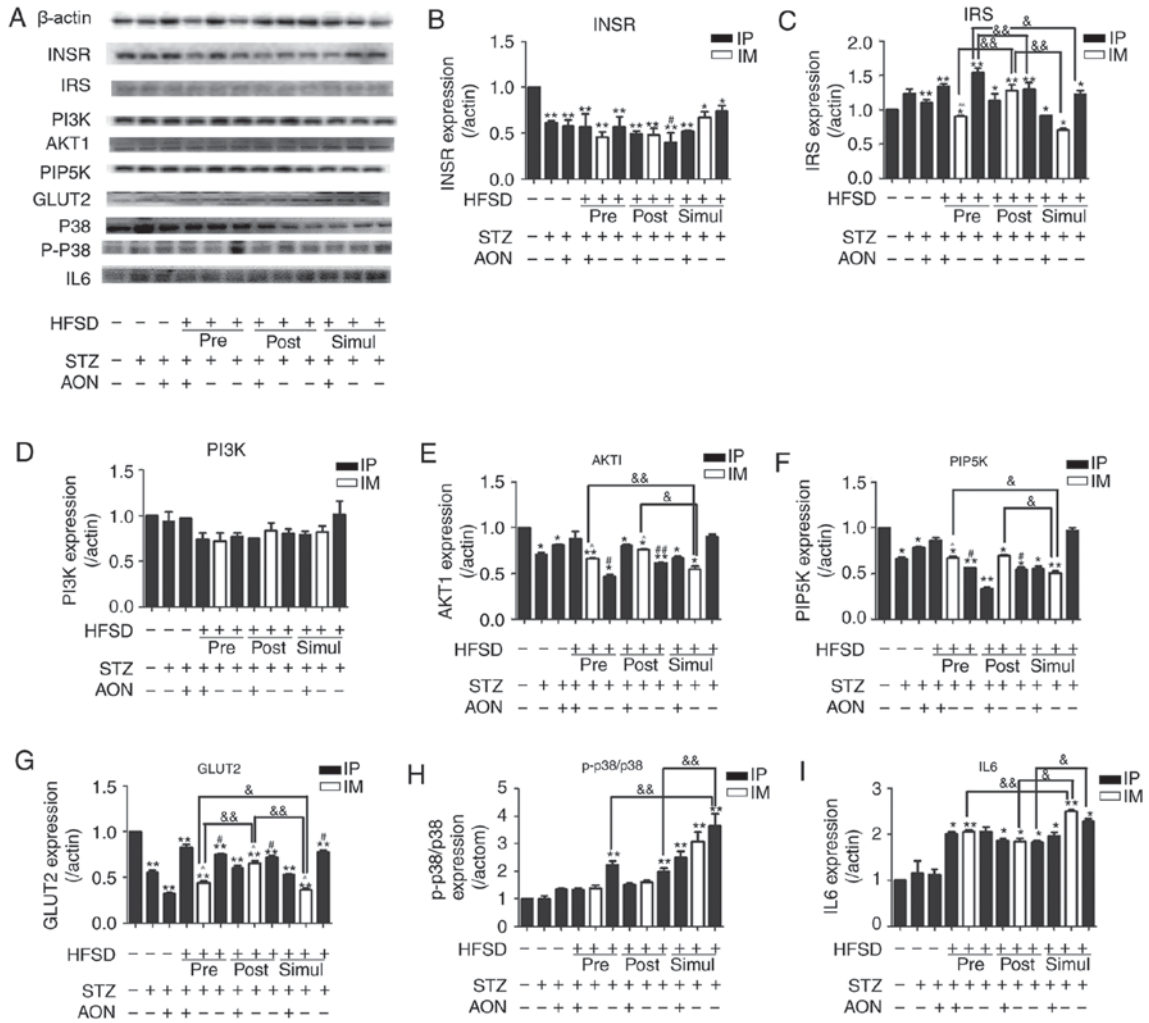

Figure 4. Protein expression levels of INSR/PI3K/AKT/GLUT2 signaling pathway factors and inflammatory cytokines in the liver. (A) Protein bands of insulin signaling pathway and inflammation. Quantified protein levels for (B) INSR, (C) IRS1, (D) PI3K, (E) AKT1, (F) PIP5K, (G) GLUT2, (H) p-p38/p38 and (I) IL6. Values are presented as the mean + standard deviation (n=10). *P<0.05 or **P<0.01 vs. control group; $^{\#}$P<0.05 or $^{\#\#}$P<0.01 vs. ND group given STZ alone; $^{\&}$P<0.05 or $^{\&\&}$P<0.01; and ^P<0.05 or ^^P<0.01 vs. HFSD groups given STZ alone via IP. IP, intraperitoneal; IM, intramuscular; ND, normal diet; AON, alloxan monohydrate; STZ, streptozotocin; HFSD, high fat and sugar diet; AKT1, protein kinase B; INSR, insulin receptor; PI3K, phosphoinositide 3-kinase; IL6, interleukin 6; GLUT2, glucose transporter 2; PIP5K, phosphatidylinositol-4-phosphate 5-kinase; IRS1, insulin receptor substrate 1; p, phosphorylated.

ratio, this difference was statistically significant (P<0.05 or P<0.01; Fig. 3A-C). Additionally, blood glucose and insulin were significantly increased in STZ pre-, post- and simul-given HFSD groups with IP STZ alone compared with the ND group given STZ alone (P<0.05 or P<0.01). Furthermore, insulin and HOMA-IR ratio in the simul-given HFSD with IM STZ group were significantly increased compared with the pre-given and post-given HFSD with IM STZ groups (P<0.05 or P<0.01; Fig. 3B and C, respectively).

Compared with the control group, blood TC, TG and LDL lipid levels in simul-given HFSD groups were significantly increased (P<0.05 or P<0.01; Fig. 3D-F). In addition, the TG levels in simul-given HFSD groups injected STZ via IM were significantly increased compared with the IM group in pre-given and post-given HFSD types (P<0.01; Fig. 3E). Additionally, HDL behaved inconsistently in model groups (Fig. 3G). These aberrations in glucose, insulin and lipid levels suggested that rat models successfully exhibited metabolic dysfunction, including hyperglycemia and hypertriglyceridemia.

Compared with STZ alone, the combination of STZ and AON indicated no significant alterations in all biochemical indexes within pre-, post- and simul-given groups. Additionally, marked differences were observed between IP and IM STZ alone in simul-given HFSD groups.

Consequently, these findings demonstrated that the majority of the model groups altered a series of biochemical indexes compared with the control group, indicating that the T2DM rat model was successfully established. Simul-given STZ HFSD groups exhibited a significant increase in all indexes vs. controls (P<0.05 or P<0.01), except HDL. Therefore, excluding the influence of combination therapy with STZ and AON on this model, subsequent research may consider the roles of other modeling factors in T2DM rat model.

Influence of constructed model groups on the INSR/PI3K/AKT/GLUT2 signaling pathway, p38 and IL6 in rat livers. The expression levels of proteins associated with the insulin signaling pathway in the liver were investigated using the established model in the present study. Fig. 4 indicated

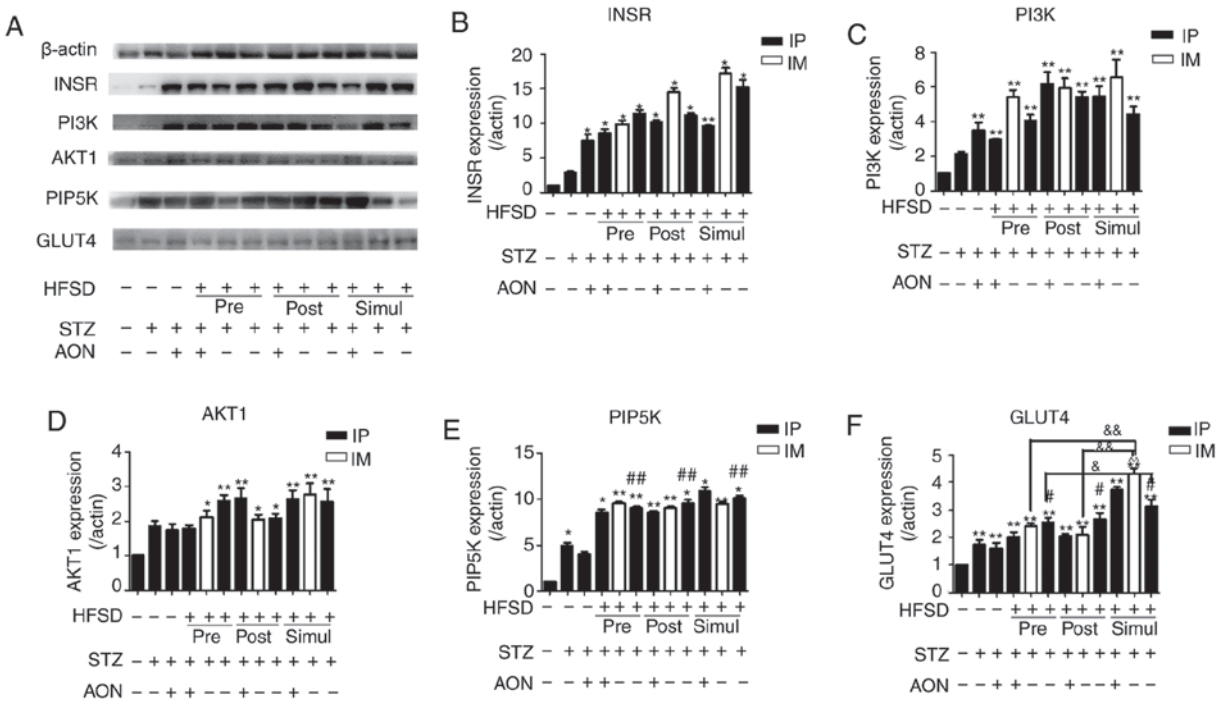

Figure 5. Protein expression levels of INSR/PI3K/AKT/GLUT4 signaling pathway mediators in the skeletal muscle. (A) Protein bands of insulin signaling pathway. Quantified protein levels for (B) INSR, (C) PI3K, (D) AKT1, (E) PIP5K and (F) GLUT4. Values are presented as the mean + standard deviation (n=10). *P<0.05 or **P<0.01 vs. control group; $^{\#}$P<0.05 or $^{\#\#}$P<0.01 vs. ND group given STZ alone; $^{\&}$P<0.05 or $^{\&\&}$P<0.01; and ^P<0.05 or ^^P<0.01 vs. HFSD groups given STZ alone via IP. IP, intraperitoneal; IM, intramuscular; ND, normal diet; AON, alloxan monohydrate; STZ, streptozotocin; HFSD, high fat and sugar diet; AKT1, protein kinase B; INSR, insulin receptor; PI3K, phosphoinositide 3-kinase; IL6, interleukin 6; GLUT4, glucose transporter 4; PIP5K, phosphatidylinositol-4-phosphate 5-kinase.

that T2DM-inducing factors decreased the protein expression levels of INSR, AKT1, PIP5K2α and GLUT2 compared with the control group. In the majority of cases the difference was statistically significant (P<0.05 or P<0.01). Conversely, IRS1 was inconsistently increased or decreased in model groups compared with the control group (Fig. 4C). Furthermore, p-p38/p38 and IL6 protein expression levels were increased in the model groups compared with the control group, and in many groups this difference was statistically significant (P<0.05 or P<0.01; Fig. 4H and I). However, there was no significant difference in model groups compared with the control group regarding PI3K expression (P>0.05; Fig. 4D).

Notably, the protein expression levels of AKT1, PIP5K2α and GLUT2 in the simul-given STZ IM-injected HFSD groups were significantly decreased compared with the respective post-given and pre-given HFSD groups (P<0.05 or P<0.01). Furthermore, protein expression levels of GLUT2 in the pre-given STZ IM-injected HFSD group were significantly decreased compared with the post-given STZ IM-injected HFSD group (P<0.05). Consistently, compared with the ND group IP administered with STZ alone, the protein expression levels of AKT1and PIP5K2α in respective pre-given and post-given HFSD IP injected STZ groups were significantly decreased (P<0.05 or P<0.01), whereas the expression of GLUT2 was significantly increased (P<0.05). The protein expression levels of p-p38/p38 in the simul-given HFSD groups administered IP STZ alone were significantly increased compared with the respective pre- and post-given HFSD groups (P<0.01). Furthermore, IL6 protein expression levels were significantly increased between the simul-given IM STZ HFSD group and the respective pre- and post-given HFSD groups (P<0.01 and P<0.05, respectively), which indicated that the inflammation level of IL6 and MAPK-p38 may be associated with the simultaneous induction of HFSD and STZ. These findings suggest that the decrease of INSR, AKT1, PIP5K2α and GLUT2 expression in the INSR/PI3K/AKT/GLUT2 signaling pathway may contribute to IR and that MAPK-p38 signaling may promote this impairment.

Influence of constructed model groups on the INSR/PI3K/AKT/GLUT4 signaling pathway in rat skeletal muscle. The protein expression levels of insulin signaling pathway mediators were investigated to evaluate IR in the skeletal muscle. Results indicated that the protein expression levels of INSR, PI3K, AKT1, PIP5K2α and GLUT4 were significantly increased in pre-, post- and simul-given HFSD groups compared with the control group (P<0.05 or P<0.01; Fig. 5), with the exception of AKT1 expression in the STZ and AON treated pre-given HFSD group. However, there was no significant difference in these protein expression levels between HFSD groups with the exception of GLUT4, where the simul-given HFSD group administered IP STZ alone expressed significantly increased levels of GLUT4 compared with the IP STZ group in pre-given HFSD type (P<0.05). Compared with the ND group injected with STZ alone, there was an observable alteration in PIP5K2α and GLUT4 in the HFSD groups treated with IP STZ alone (P<0.05 or P<0.01), which suggests that HFSD may simultaneously increase these proteins in this T2DM model. Furthermore, these results indicate that the expression of factors associated with the insulin

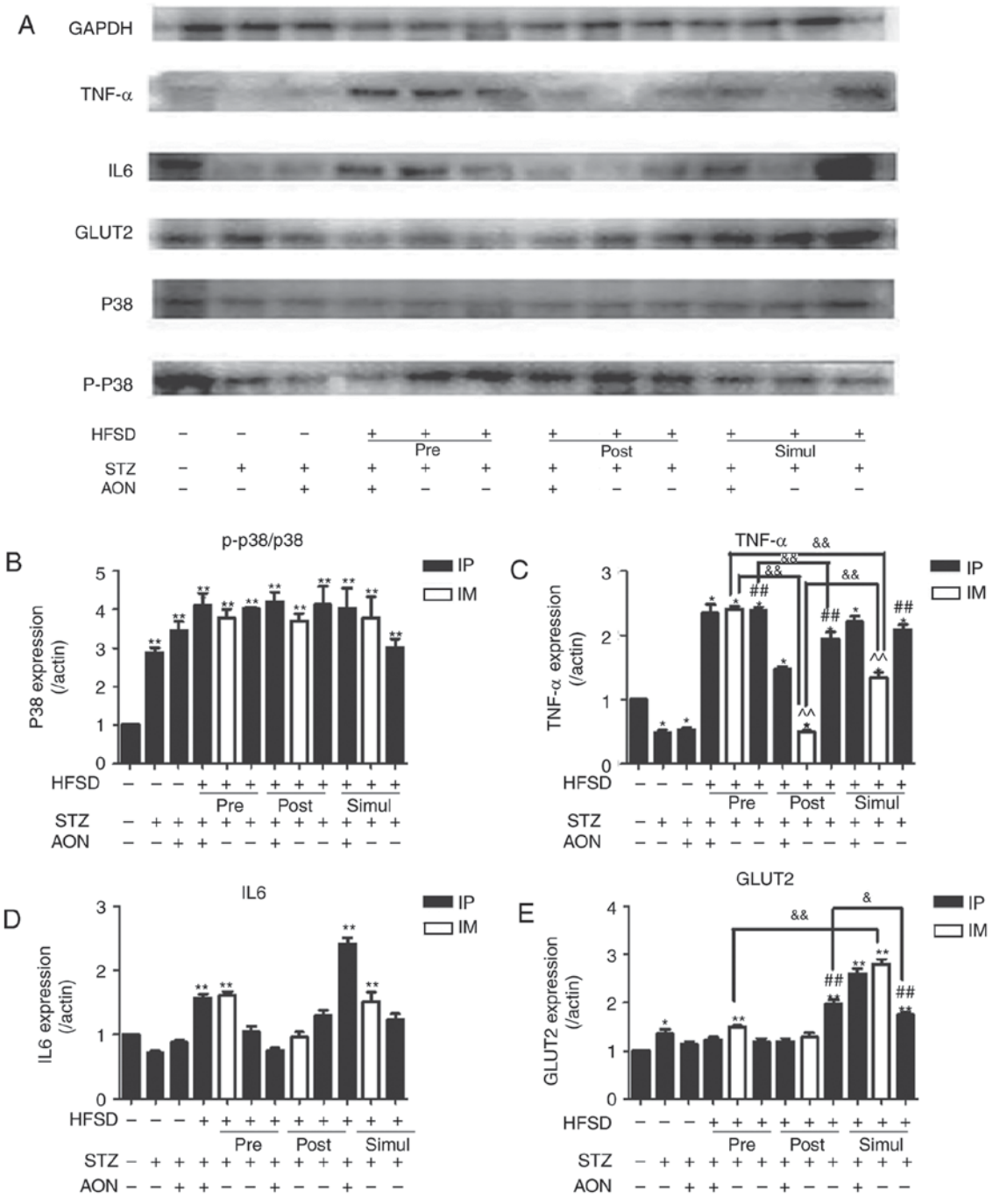

Figure 6. Impact of type 2 diabetes mellitus models on inflammation and GLUT2 expression levels in the pancreas. (A) Protein bands of insulin signaling pathway and inflammation. Quantified protein levels for (B) p-p38/p38, (C) TNF, (D) IL6 and (E) GLUT2. Values are presented as the mean + standard deviation (n=10). *P<0.05 or **P<0.01 vs. control group; $^{\#}$P<0.05 or $^{\#\#}$P<0.01 vs. ND group given STZ alone; $^{\&}$P<0.05 or $^{\&\&}$P<0.01; and ^P<0.05 or ^^P<0.01 vs. HFSD groups given STZ alone via IP. IP, intraperitoneal; IM, intramuscular; ND, normal diet; AON, alloxan monohydrate; STZ, streptozotocin; HFSD, high fat and sugar diet; IL6, interleukin 6; GLUT2, glucose transporter 2; PIP5K, phosphatidylinositol-4-phosphate 5-kinase; IRS, insulin receptor substrate 1; TNF, tumor necrosis factor; p, phosphorylated.

signaling pathway in the skeletal muscle are not significantly affected by IR; therefore, the present T2DM model may not be eligible to investigate IR in skeletal muscle.

Influence of constructed model groups on inflammation in pancreas. Protein expression levels of MAPK-p38 signaling mediators and inflammatory cytokines were evaluated in the pancreas of rats. As indicated in Fig. 6, compared with the control group, the results indicated that the protein expression levels of p-38/p38 and TNFα exhibited significant differences in the majority of the model groups, and in a minority of groups regarding IL6 and GLUT2 expression (P<0.05 or P<0.01). Notably, compared with the control group, GLUT2 expression levels were significantly increased in all simul-given HFSD groups (P<0.01). In addition, compared with ND group administered STZ alone, GLUT2 expression levels were significantly

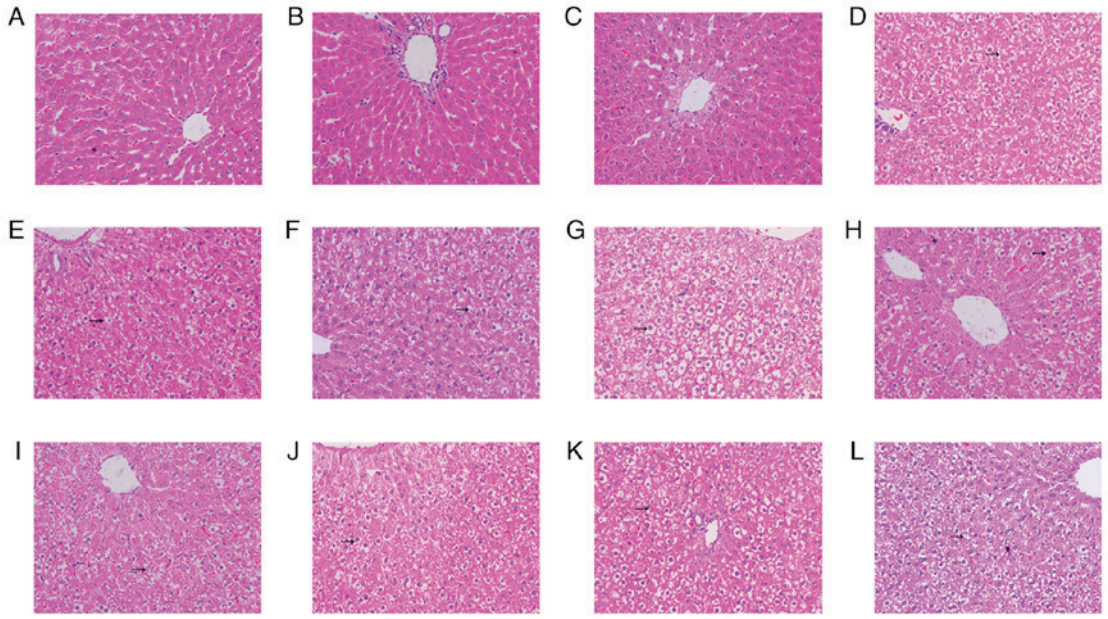

Figure 7. Hematoxylin and eosin staining from the liver tissue of type 2 diabetes mellitus model rats. All images are presented at a magnification of x200. Liver tissue of the (A) control group, (B) ND group given STZ via IP injection, (C) ND group given STZ and AON via IP injection, (D) HFSD group pre-given plus STZ and AON via IP injection, (E) HFSD group pre-given plus STZ via IM injection, (F) HFSD group pre-given plus STZ via IP injection, (G) HFSD group post-given plus STZ and AON via IP injection, (H) HFSD group post-given plus STZ via IM injection, (I) HFSD group post-given plus STZ via IP injection, (J) HFSD group simul-given plus STZ and AON via IM injection, (K) HFSD group simul-given plus STZ via IP injection and (L) HFSD group simul-given plus STZ via IM injection. IP, intraperitoneal; IM, intramuscular; ND, normal diet; AON, alloxan monohydrate; STZ, streptozotocin; HFSD, high fat and sugar diet.

increased in the simul- and post-given HFSD groups that received IP injections with STZ alone ($P<0.01$). Similar results were also observed for TNFα expression levels. These findings suggest that inflammation of the pancreas may be associated with an HFSD.

Histopathological changes in the liver of T2DM rats. Hepatocytes of the control, ND IP injection with STZ alone and ND IP injection with STZ and AON groups indicated regular hexagon-like shaped liver lobules with similar sized nuclei (Fig. 7A-C). The hepatocytes were presented in a rope-like distribution and the binding between each chain was obvious. In addition, there was obvious hepatic sinusoid between the rope-like chain of hepatocytes. There was no observable limit of air quality vesicles in the cytoplasm, which was uniformly stained. Additionally, the blue-stained nuclei were located medially. However, compared with ND groups, in the groups administered STZ plus HFSD (Fig. 7D-L), a number of air quality vesicles were observed, which were of different sizes and possessed clear limits in livers from HFSD-fed rats. The variation of hepatocyte size markedly increased following long-term administration of HFSD, and nuclear shrinkage was also observed.

Histopathological changes in the pancreas of T2DM rats. H&E staining of pancreatic tissue indicated that the normal islet cells presented as an ellipse with a clear boundary in the control group (Fig. 8A). There were numerous stable trials with normal islet cells, including the integrity of nuclear, obvious cell structure and non-vacuolation. Compared with the control group, the number of islet cells in STZ plus HFSD groups (Fig. 8D-L) was markedly decreased, the shape was irregular and boundaries were unclear. Furthermore, in STZ plus HFSD groups the nuclei were smaller, vacuolation occurred in the cytoplasm, part of cells had become swollen and denaturation was observed.

Discussion

Insulin not only regulates glucose metabolism but also has a vital role in lipid metabolism (20,21). Consequently, insulin deficiency is likely to induce dysfunction of these metabolic processes, which in turn promotes IR (22).

The mechanism of insulin resistance induced by HFSD plus agents is depicted in Fig. 9. Previous findings have suggested that excess accumulation of lipids trigger the MAPK signaling pathway (23), which leads to increased secretion of inflammatory cytokines, including TNFα and IL6, which are associated with attacking the islet cells and interfering with the insulin signal pathway, subsequently lessening the efficiency of glucose uptake (15). Therefore, inflammatory cytokines may be a risk factor to consider in the pathogenesis of IR. Previous pathological results have indicated that, compared with control group and ND groups in liver and pancreatic tissues, a large number of lipid droplets invaded in groups subjected to a HFSD (23). In the present study, protein expression levels of p38, p-p38, TNFα and IL6 were also increased in HFSD groups, which suggests that a prolonged HFSD may render organ fat pathological changes and promote an inflammatory response.

It is acknowledged that INSR/PI3K/AKT/GLUT signaling is primarily associated with insulin signaling in the skeletal muscle and liver (24). Additionally, this pathway has been suggested to be a major mechanism in the development of IR (25). INSR is susceptible to insulin and the down-stream protein IRS1 is associated with tyrosine phosphorylation,

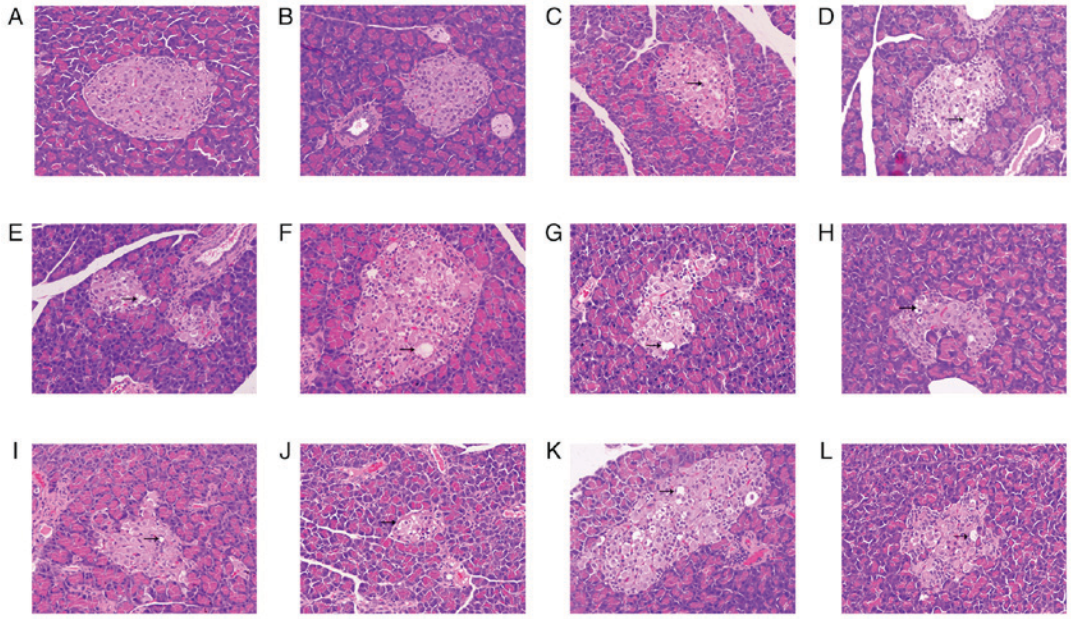

Figure 8. Hematoxylin and eosin staining from the pancreatic tissue of type 2 diabetes mellitus model rats. All images are presented at a magnification of x200. Pancreatic tissue of the (A) control group, (B) ND group given STZ via IP injection, (C) ND group given STZ and AON via IP injection, (D) HFSD group pre-given plus STZ and AON via IP injection, (E) HFSD group pre-given plus STZ via IM injection, (F) HFSD group pre-given plus STZ via IP injection, (G) HFSD group post-given plus STZ and AON via IP injection, (H) HFSD group post-given plus STZ via IM injection, (I) HFSD group post-given plus STZ via IP injection, (J) HFSD group simul-given plus STZ and AON via IM injection, (K) HFSD group simul-given plus STZ via IP injection and (L) HFSD group simul-given plus STZ via IM. IP, intraperitoneal; IM, intramuscular; ND, normal diet; AON, alloxan monohydrate; STZ, streptozotocin; HFSD, high fat and sugar diet.

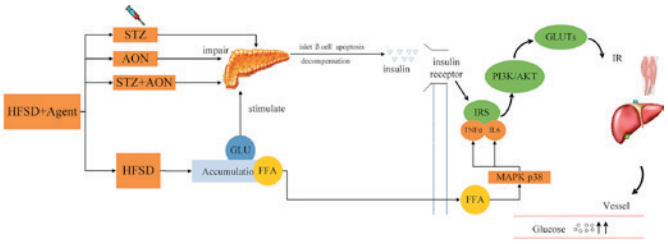

Figure 9. Mechanism of insulin resistance induced by HFSD plus agents. HFSD may render toxic accumulation by promoting excessive production of FFA and removal of glucose in the blood, triggering the p38 inflammation signaling pathway to release TNFα and IL6, which may interfere with IRS regular phosphorylation, reduce PI3K/AKT signaling pathway activity and failure of GLUTs expression. Otherwise, HFSD is able to induce compensated secretion of insulin, as its function has been impaired, which may lead to insulin deficiency. In addition, STZ and AON are able to destroy some islet β cells which may result in a deficiency of insulin. IP, intraperitoneal; IM, intramuscular; ND, normal diet; AON, alloxan monohydrate; STZ, streptozotocin; HFSD, high fat and sugar diet; GLU, glucose; FFA, free fatty acid; MAPK, mitogen-activated protein kinase; TNFα, tumor necrosis factor α; IL6, interleukin 6; IRS, insulin receptor substrate 1; PI3K, phosphoinositide 3-kinase; GLUTs, glucose transporters; IR, insulin resistance.

which activates PI3K (26). The activation of PI3K initiates AKT, which upregulates the expression levels of PIP5K2α, and PIP5K2α, resulting in the translocation of GLUTs into the membrane to initiate glucose uptake (27). Therefore, any alteration of protein expression in this stream may influence the sensitivity of insulin.

A decrease of INSR, AKT1, PIP5K2α and GLUT2 expression, as well as a significant increase in IL6 in the liver tissue of HFSD groups that received IM injections with STZ was observed in the present study compared with the control group. Apart from INSR, these alterations of proteins were more marked in the simul-given group, further suggesting that the reduced sensitivity of insulin was attributed to decreased insulin signaling and activation of inflammation. Conversely, GLUT2 in the pancreas was elevated following the simultaneous induction of modeling agents and HFSD, probably attributing to its immediate coping mechanism (28). Interestingly, in all ND and HFSD groups, protein expression of GLUT4 in skeletal muscle did not appear to be affected by IR, which differed from previous research results (29,30). These findings suggest that further study is required to fully elucidate the mechanism associated with IR. Notably, a previous study indicated that GLUT2 in liver tissue, where a high level of glucose is typically observed, presented a low expression in response to IR stress (31).

The present findings suggest that irregular and prolonged HFSD diet styles may negatively impact INSR/PI3K/AKT signaling and promote inflammation. These consequences of the signaling pathway and inflammation suggest that the diet may be a useful indicator of IR. In the present study, HFSD and IM STZ were simultaneously administered to establish a T2DM rat model. The results indicated that the most stable T2DM rat model can be further verified by actions of insulin signaling pathway and MAPK pathway.

It has been reported that low dosage of STZ (35 mg/kg) is able to destroy parts of islet β cells to reduce the production of insulin rather than to a completely destructive degree, and AON is known to influence the permeability and production of ATP in islet β cells (32). In regards to weight, liver ratio and pancreas ratio, there was no significant difference among HFSD groups in the present study, however, significant differences were observed in HFSD groups compared with

the control group, which suggests the influence on above indexes may be due to HFSD. However, administration with STZ alone and the combination of STZ and AON in ND or HFSD groups were not significantly different with respect to glucose, insulin level, and protein expression levels of insulin signaling pathway and inflammation, although each were significantly different compared with controls. The present findings therefore indicate that administration with STZ alone is sufficient to establish the T2DM model, and more efficient than combination treatment.

Compared with the ND group administered with STZ alone, increased glucose, insulin and lipid levels including TC, TG, LDL and HDL in the HFSD simul-given types, were observed. Furthermore, staining results of liver and pancreatic tissues indicated inflammation and air quality vesicles were present in HFSD simul-given rats, which was likely due to more serious dysfunction of glycolipid induced by STZ and prolonged HFSD simultaneously (33). The present findings indicated that the HFSD simul-given rats exhibited the pathological traits of T2DM, both dyslipidemia and hyperglycemia, which was not observed to the same extent in the other HFSD types. Additionally, based on advantages HFSD simul-given possessed, following comparisons in this type of HFSD from biochemical indexes, the majority of indexes were not significantly different between the IM and IP-administered STZ simul-given groups, although the level of insulin in the IM group was significantly higher than in the IP group. Furthermore, the present results demonstrated that protein expression levels of GLUT2 in HFSD groups that received IM administration of STZ in the liver were significantly different compared with alterations that occurred in HFSD group that received IP injection with STZ alone, which suggests that the injection routes may influence the T2DM model.

In conclusion, the present findings indicated that the modeling effect of STZ injection alone provided a similar effect as the combination of STZ with AON, however, the former is more economical and controlled compared with the latter. Additionally, based on efficacy of modeling, administration of STZ via IM is notably different than injection via IP for certain indexes detailed above, including enhanced insulin level and reduced TNFα expression in pancreas. The findings of the present study evaluated the content of pathological situation in T2DM models and elucidated the effect of STZ and an HFSD on key proteins associated with the INSR/PI3K/AKT signaling pathway. Furthermore, the present study results may benefit further research on T2DM pathogenesis and the identification of potential therapeutic targets.

Acknowledgements

The present study was supported by Ministry of Science and Technology of PRC (grant no. 2016ZX09101076), Natural Science Foundation of Guangdong Province (grant no. S2013010012360), Guangdong Provincial Department of Science and Technology (grant nos. 2013B060300034, 2014A070705014 and 2015A040404030), Administration of Traditional Chinese Medicine of Guangdong Province (grant nos. 20141028, 20151013, 20152006 and 20161026) and Guangdong Provincial key Laboratory of Research and Development in Traditional Chinese Medicine.

Competing interests

The authors declare that they have no competing interests.

References

1. Chang WC, Wu JS, Chen CW, Kuo PL, Chien HM, Wang YT and Shen SC: Protective effect of vanillic acid against hyperinsulinemia, hyperglycemia and hyperlipidemia via alleviating hepatic insulin resistance and inflammation in high-fat diet (HFD)-Fed rats. Nutrients 7: 9946-9959, 2015.
2. Global Burden of Disease Study 2013 Collaborators: Global, regional, and national incidence, prevalence, and years lived with disability for 301 acute and chronic diseases and injuries in 188 countries, 1990-2013: A systematic analysis for the Global Burden of Disease Study 2013. Lancet 386: 743-800, 2015.
3. Levey AS and Coresh J: Chronic kidney disease. Lancet 379: 165-180, 2012.
4. Sabanayagam C, Yip W, Ting DS, Tan G and Wong TY: Ten emerging trends in the epidemiology of diabetic retinopathy. Ophthalmic Epidemiol 23: 209-222, 2016.
5. Qian J, Thomas AP, Schroeder AM, Rakshit K, Colwell CS and Matveyenko AV: Development of diabetes does not alter behavioral and molecular circadian rhythms in a transgenic rat model of type 2 diabetes mellitus. Am J Physiol Endocrinol Metab 313: E213-E221, 2017.
6. 6. Li N, Liu Q, Li XJ, Bai XH, Liu YY, Jin ZY, Jing YX, Yan ZY and Chen JX: Establishment and evaluation of a rat model of type 2 diabetes associated with depression. Zhongguo Ying Yong Sheng Li Xue Za Zhi 31: 23-26, 2015 (In Chinese).
7. Fatih Aydın A, Küçükgergin C, Bingül İ, Doğan-Ekici I, Doğru-Abbasoğlu S and Uysal M: Effect of Carnosine on renal function, oxidation and glycation products in the kidneys of high-fat diet/streptozotocin-induced diabetic rats. Exp Clin Endocrinol Diabetes 125: 282-289, 2017.
8. Liu XY, Liu FC, Deng CY, Zhang MZ, Yang M, Xiao DZ, Lin QX, Cai ST, Kuang SJ, *et al*: Left ventricular deformation associated with cardiomyocyte Ca(2+) transients delay in early stage of low-dose of STZ and high-fat diet induced type 2 diabetic rats. BMC Cardiovasc Disord 16: 41, 2016.
9. Ma YG, Zhang YB, Bai YG, Dai ZJ, Liang L, Liu M, Xie MJ and Guan HT: Berberine alleviates the cerebrovascular contractility in streptozotocin-induced diabetic rats through modulation of intracellular Ca^{2+} handling in smooth muscle cells. Cardiovasc Diabetol 15: 63, 2016.
10. Andrade EF, Lima AR, Nunes IE, Orlando DR, Gondim PN, Zangeronimo MG, Alves FH and Pereira LJ: Exercise and Beta-Glucan consumption (Saccharomyces cerevisiae) improve the metabolic profile and reduce the atherogenic index in Type 2 diabetic rats (HFD/STZ). Nutrients 8: E792, 2016.
11. Li Y, Zhang T, Zhang X, Zou W, Gong X and Fu J: Cinepazide maleate improves cognitive function and protects hippocampal neurons in diabetic rats with chronic cerebral hypoperfusion. Biol Pharm Bull 40: 249-255, 2017.
12. Bolzán AD and Bianchi MS: Genotoxicity of streptozotocin. Mutat Res 512: 121-134, 2002.
13. Xiao X, Xu L, Zhu L and Ding Q: Study on the model of diabetic mice and rat induced by Alloxan. Science Mosaic 7: 112-114, 2010.
14. Hu C, Zhang G, Sun D, Han H and Hu S: Duodenal-jejunal bypass improves glucose metabolism and adipokine expression independently of weight loss in a diabetic rat model. Obes Surg 23: 1436-1444, 2013.
15. Yu X, Shen N, Zhang ML, Pan FY, Wang C, Jia WP, Liu C, Gao Q, Gao X, Xue B and Li CJ: Egr-1 decreases adipocyte insulin sensitivity by tilting PI3K/Akt and MAPK signal balance in mice. EMBO J 30: 3754-3765, 2011.
16. Dai B, Wu Q, Zeng C, Zhang J, Cao L, Xiao Z and Yang M: The effect of Liuwei Dihuang decoction on PI3K/Akt signaling pathway in liver of type 2 diabetes mellitus (T2DM) rats with insulin resistance. J Ethnopharmacol 192: 382-389, 2012.
17. Antony PJ, Gandhi GR, Stalin A, Balakrishna K, Toppo E, Sivasankaran K, Ignacimuthu S and Al-Dhabi NA: Myoinositol ameliorates high-fat diet and streptozotocin-induced diabetes in rats through promoting insulin receptor signaling. Biomed Pharmacother 88: 1098-1113, 2017.

18. Zouari R, Hamden K, Feki AE, Chaabouni K, Makni-Ayadi F, Kallel C, Sallemi F, Ellouze-Chaabouni S and Ghribi-Aydi D: Protective and curative effects of Bacillus subtilis SPB1 biosurfactant on high-fat-high-fructose diet induced hyperlipidemia, hypertriglyceridemia and deterioration of liver function in rats. Biomed Pharmacother 84: 323-329, 2016.
19. International Guiding Principles for Biomedical Research Involving Animals issued by CIOMS. Vet Q 8: 350-352, 1986.
20. Feng W, Zhao T, Mao G, Wang W, Feng Y, Li F, Zheng D, Wu H, Jin D, Yang L and Wu X: Type 2 diabetic rats on diet supplemented with chromium malate show improved glycometabolism, glycometabolism-related enzyme levels and lipid metabolism. PLoS One 10: e125952, 2015.
21. Smith U and Kahn BB: Adipose tissue regulates insulin sensitivity: Role of adipogenesis, de novo lipogenesis and novel lipids. J Intern Med 280: 465-475, 2016.
22. Wu Y, Wu T, Wu J, Zhao L, Li Q, Varghese Z, Moorhead JF, Powis SH, Chen Y and Ruan XZ: Chronic inflammation exacerbates glucose metabolism disorders in C57BL/6J mice fed with high-fat diet. J Endocrinol 219: 195-204, 2013.
23. Savary S, Trompier D, Andréoletti P, Le Borgne F, Demarquoy J and Lizard G: Fatty acids - induced lipotoxicity and inflammation. Curr Drug Metab 13: 1358-1370, 2012.
24. Gao Y, Zhang M, Wu T, Xu M, Cai H and Zhang Z: Effects of D-Pinitol on insulin resistance through the PI3K/Akt signaling pathway in Type 2 diabetes mellitus rats. J Agric Food Chem 63: 6019-6026, 2015.
25. Yang M, Ren Y, Lin Z, Tang C, Jia Y, Lai Y, Zhou T, Wu S, Liu H, Yang G and Li L: Krüppel-like factor 14 increases insulin sensitivity through activation of PI3K/Akt signal pathway. Cell Signal 27: 2201-2208, 2015.
26. Gao TT, Qin ZL, Ren H, Zhao P and Qi ZT: Inhibition of IRS-1 by hepatitis C virus infection leads to insulin resistance in a PTEN-dependent manner. Virol J 12: 12, 2015.
27. Liu T, Yu B, Kakino M, Fujimoto H, Ando Y, Hakuno F and Takahashi SI: A novel IRS-1-associated protein, DGKzeta regulates GLUT4 translocation in 3T3-L1 adipocytes. Sci Rep 6: 35438, 2016.
28. Bae JS, Kim TH, Kim MY, Park JM and Ahn YH: Transcriptional regulation of glucose sensors in pancreatic beta-cells and liver: An update. Sensors (Basel) 10: 5031-5053, 2010.
29. Garvey WT, Maianu L, Hancock JA, Golichowski AM and Baron A: Gene expression of GLUT4 in skeletal muscle from insulin-resistant patients with obesity, IGT, GDM, and NIDDM. Diabetes 41: 465-475, 1992.
30. Zorzano A, Palacin M and Gumà A: Mechanisms regulating GLUT4 glucose transporter expression and glucose transport in skeletal muscle. Acta Physiol Scand 183: 43-58, 2005.
31. Narasimhan A, Chinnaiyan M and Karundevi B: Ferulic acid regulates hepatic GLUT2 gene expression in high fat and fructose-induced type-2 diabetic adult male rat. Eur J Pharmacol 761: 391-397, 2015.
32. Bloch KO, Zemel R, Bloch OV, Grief H and Vardi P: Streptozotocin and alloxan-based selection improves toxin resistance of insulin-producing RINm cells. Int J Exp Diabetes Res 1: 211-219, 2000.
33. Erion DM, Park HJ and Lee HY: The role of lipids in the pathogenesis and treatment of type 2 diabetes and associated co-morbidities. BMB Rep 49: 139-148, 2016.